Journal of Power Sources 196 (2011) 2802–2809

Contents lists available at ScienceDirect

Journal of Power Sources

journal homepage: www.elsevier.com/locate/jpowsour

High discharge capacity solid composite polymer electrolyte lithium battery

Y.T. Chen, Y.C. Chuang, J.H. Su, H.C. Yu, Y.W. Chen-Yang*

Department of Chemistry and Center for Nanotechnology, Chung Yuan Christian University, 200 Chung-Pei Road, Chung-Li 32023, Taiwan, ROC

ARTICLE INFO

Article history:
Received 24 July 2010
Received in revised form 5 November 2010
Accepted 9 November 2010
Available online 16 November 2010

Keywords:
Solid composite polymer electrolyte
Silica aerogel
Discharge capacity
Ionic conductivity
Lithium battery

ABSTRACT

In this study, a series of nanocomposite polymer electrolytes (CPEs), PAN/$LiClO_4$/SAP, with high conductivity are prepared based on polyacrylonitrile (PAN), $LiClO_4$ and low content of the silica aerogel powder (SAP) prepared by the sol–gel method with ionic liquid (IL) as the template. The effect of addition of SAP on the properties of the CPEs is investigated by FTIR, AC impedance, linear sweep voltagrams and cyclic voltammetry measurements as well as the charge–discharge performance. It is found that the ionic conductivity of the CPE is significantly improved by addition of SAP. The maximum ambient ionic conductivity of CPEs is about 12.5 times higher than that without addition of SAP. The results of the voltammetry measurements of CPE-3, which contained 3 wt% of SAP, show that the anodic and cathodic peaks are well maintained after 100 cycles, showing excellent electrochemical stability and cyclability over the potential range between 0 V and 4 V vs. Li/Li^+. Besides, the room temperature discharge capacity measured at 0.5C for the coin cell based on CPE-3 is 120 mAh g^{-1} and the capacity is retained after 20 cycles discharge, indicating the potential for practical use. This is perhaps the first report of the room temperature charge–discharge performance on the solid composite polymer electrolyte to the best of our knowledge.

1. Introduction

In recent years, lithium batteries played a key role in the storage of intermittent energy sources, including solar or wind, as well as in the powering of controlled emission, electric or hybrid vehicles. However, most of the lithium batteries which composed of liquid electrolyte or gel electrolyte have suffered poor mechanical property and the possible hazard caused by the organic solvent incorporated and a progressive evaporation of excess liquid solvent, which may induce a progressive decrease in the ionic conductivity [1]. In order to solve these problems, solid polymer electrolytes have been suggested. Nevertheless, most of the solid polymer electrolytes reported had several disadvantages, which limit their commercial applications. One major drawback is their relatively low ionic conductivity at ambient temperature. Several approaches have been applied to improve their room temperature ionic conductivity [2]. One of the most successful approaches to improve it is to prepare the composite polymer electrolytes (CPEs) by addition of inorganic fillers, which include ceramics [1,3–9], layer clays [10–12], organic–inorganic hybrid materials [13,14] and mesoporous materials [15–20]. The results showed that addition of the inorganic fillers has improved many properties of the polymer electrolytes, such as ionic conductivity, lithium ion transference number (t^+), mechanical properties, and the stability of electrolyte–electrode interface. These improvements have been ascribed to the fillers that (1) acted as the plasticizers and lowered the crystalline of the polymer matrix [21], (2) increased ion mobility by providing additional conductive pathway due to formation of the Lewis acid–base interactions [22], and (3) increased the number of charge carriers due to enhancement of the salt dissociation [23]. Besides, it was found that the conductivity of CPE was varied with the morphology of the filler. For example, compared to the non-porous particle fillers, the corresponding mesoporous fillers usually showed larger enhancement on its conductivity in the CPEs due to its higher surface area [17,18] and the larger pores, facilitating the intercalation of the polymer chains [24]. However, the conductivities and other related properties reported are still not high enough for practical application. Therefore, finding new filler, which can enhance the electrochemical properties of the solid polymer electrolyte and the corresponding lithium battery performance, is still an attractive topic.

Silica aerogel is a tunable and designable material which possesses unique properties and features [25], such as low density (0.003–0.5 g cm^{-3}), high porosity (90–99%), large surface area (>800 m^2 g^{-1}) and interconnected pores and has been employed in many applications [26]. In our previous studies [19], we found that with addition of the silica aerogel powder (SAP) prepared the ionic conductivity, cation transference and other related properties of the PEO-based polymer composite electrolyte for lithium battery were significantly increased. Nevertheless, the charge–discharge

* Corresponding author. Tel.: +886 3 265 3317; fax: +886 3 265 3399.
E-mail address: yuiwhei@cycu.edu.tw (Y.W. Chen-Yang).

0378-7753/$ – see front matter © 2010 Elsevier B.V. All rights reserved.
doi:10.1016/j.jpowsour.2010.11.058

Table 1
Compositions and abbreviations of the composites.

	PAN (g)	$LiClO_4$ (g)	SAP (wt%)
CPE-0	0.20	0.241	0
CPE-1	0.20	0.241	1
CPE-2	0.20	0.241	2
CPE-3	0.20	0.241	3
CPE-4	0.20	0.241	4
CP-3	0.20	0	3

capacities of the lithium battery fabricated with the solid composite polymer electrolyte was unable to be measured at room temperature due to the low conductivity and mechanical property. In fact, to the best of our knowledge, none of the charge–discharge capacity has been reported for the solid polymer electrolyte lithium battery at room temperature.

In this study, silica aerogel powder (SAP) was prepared by sol–gel polymerization method as described previously [19]. The as-prepared SAP was used as a filler to prepare a series of PAN-based CPEs with $LiClO_4$. It was anticipated that the interconnected pores of SAP and the amorphous PAN matrix would provide shorter ion transport paths, resulting in higher conductivity, better compatibility with the electrodes, enhancing the cyclability and better mechanical property. Therefore, the effect of addition of SAP on the ionic conductivity and electrochemical property of the CPEs were studied. Furthermore, the charge–discharge capacities of the lithium batteries fabricated with the as-prepared CPEs as the solid composite polymer electrolytes have also been investigated.

2. Experiment

2.1. Material

Polyacrylonitrile (PAN, Mw: 150,000, Sp2), lithium perchlorate ($LiClO_4$) (reagent grade), and dimethylformamide (DMF) were purchased from Aldrich. $LiClO_4$ was dried under vacuum (<10^{-3} Torr) for 24 h at 140 °C before use. The silica aerogel powder (SAP) was prepared according to the method reported by us previously [19]. The surface area, pore diameter and pore volume of SAP measure was 619 $m^2\,g^{-1}$, 7.0 nm and 1.2 $cm^3\,g^{-1}$, respectively. The $LiFePO_4$ electrode used in the coin cell for the charge/discharge measurement was provided by Tatung Fine Chemicals Company, Taiwan and used as received.

2.2. Preparation of the composite polymer electrolytes (CPEs)

To prepare the PAN/$LiClO_4$/SAP composite polymer electrolyte (CPE), 0.200 g of PAN was first dissolved with a small amount of DMF. Then, 0.241 g of lithium salt, $LiClO_4$, was added, and the solution was well stirred. A designated amount of SAP was then added and the PAN/$LiClO_4$/SAP solution was further sonicated for 15 min using an ultrasound bath by Delta D200H to disperse the SAP particles. The solution was later cast on a flat glass slide and dried in a vacuum oven at 80 °C for at least 24 h to remove the solvent. The average thickness of the polymer electrolyte membranes was about 150 μm. In the rest of this study, CPE-*x* is used as the abbreviation of the polymer electrolyte sample containing *x* wt% of SAP. The compositions and the abbreviations of CPEs and CPs are listed in Table 1.

2.3. Instruments

2.3.1. Characterization

The ionic conductivities of the composite polymer electrolytes were measured by the AC impedance method in the temperature ranging from 30 °C to 80 °C. The samples were sandwiched between stainless steel blocking electrodes and placed in a temperature-controlled oven at vacuum (<10^{-2} Torr) for 2 h before measurement. The experiments were performed in a constant area cylindrical cell of an electrode diameter of 1.76 cm^2. The impedance measurements were carried out on a computer interfaced with an HP 4192A impedance analyzer over the frequency range of 5 Hz to 13 MHz.

The FT-IR spectra of the CPEs were recorded on a Bio-Rad FTS-7 (Bio-Rad Instruments, USA) with a wave number resolution of 2 cm^{-1}. For preparation of the sample, the corresponding PAN/$LiClO_4$/SAP solution prepared as described in the last paragraph was cast onto a KBr disk and the solvent was removed under vacuum at 80 °C for 24 h then stored in the dry box for 2 h before measurement.

High-resolution solid-state ^7Li NMR spectra were recorded on a Bruker DSX-400 spectrometer (Bruker Instruments, Billerica, MA, USA) at a resonance frequency of 155.5 MHz. The chemical shifts were externally referenced to the solution of LiCl at 0.0 ppm. For preparation of the measurement specimen, some NaCl was mixed with small amount of the cut tiny fragments sample to increase its weight in the sample tube, meeting the handling requirement.

2.3.2. Mechanical property

The mechanical properties of CPE-0 and CPE-3 were measured using a tensile tester (Q-test) equipped with a 100-N load cell and interfaced with a computer for data collection. According to ASTM D638 standard, the specimens used had dimensions of 150 mm × 15 mm × 2 mm, and the test speed was 2 in. min^{-1}.

2.3.3. Electrochemical property

The electrochemical properties of the as-prepared composite polymer electrolyte films were studied by the linear sweep voltammetry and cyclic voltammetry measurements on a three-electrode cell, in which the Pt plate employed as the working electrode and the lithium metals served as the counter and reference electrode was mounted on the SS substrate, individually, in the cell. The cell was put in a dry box filled with argon gas. The linear sweep was run from 2.5 V to 6.0 V (vs. Li/Li^+) and the cyclic voltammetry potential range was 0–4 V (vs. Li/Li^+) at a scan rate of 10 mV s^{-1}.

The charge–discharge abilities of CPE-*x* were investigated with the coin cells composed of Li metal, CPE-*x* and $LiFePO_4$ (Li/CPE-*x*/$LiFePO_4$). The cells used were coin type cells (2032) and constructed in an argon filled glove box using a coin cell crimping machine (LE-2032, Hao Ju Comp., Taiwan). Electrochemical measurement was carried out using a MACCOR 2200system (MACCOR, Inc. Tulsa, Oklahoma, USA). The assembled coin cell was subjected to preconditioning with a cut-off voltage of 4.2 V for the upper limit and 2.5 V for the lower limit at a charge rate of 0.5 C for twenty cycles.

3. Results and discussions

3.1. Ionic conductivity

Generally, the ionic conductivity of an electrolyte, σ, relates to the number of the charge carriers and their mobility in the electrolyte and is often defined as follows:

$$\sigma = \sum n_i z_i \mu_i$$

where n_i, z_i, and μ_i refer to the number of charge carriers, the ionic charge, and the ionic mobility, respectively. The ionic conductivities of the as-prepared CPEs measured by the AC impedance measurement at 30 °C vs. the SAP content are shown in Fig. 1. It shows that the ionic conductivity of the PAN-based electrolytes without SAP (CPE-0) was 4.8×10^{-5} S cm^{-1}. The conductivity increased

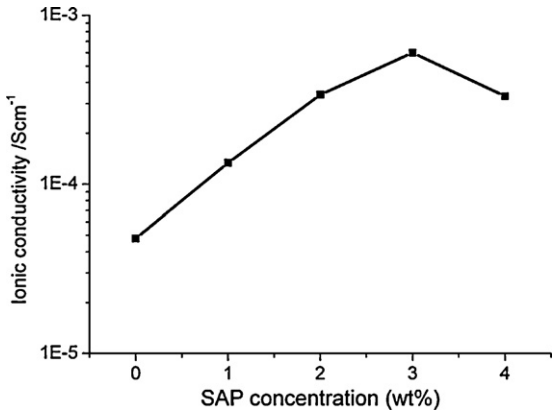

Fig. 1. Ionic conductivity of CPE vs. SAP concentration.

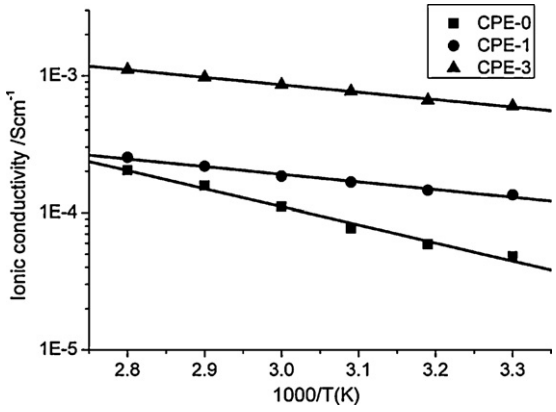

Fig. 2. Arrhenius plots of ionic conductivities of CPE-0, CPE-1 and CPE-3.

with increase of the SAP content up to 3 wt%. The maximum value of conductivity obtained from CPE-3 was 6.0×10^{-4} S cm^{-1}, which was about 12.5 times higher than that obtained from CPE-0, suggesting that addition of 3 wt% SAP content provided the most suitable environment for the ionic transport and achieved the highest conductivity. However, an excess of the SAP content resulted in decreasing the ionic conductivity. This is attributed to the aggregation of the higher loaded SAP particles, reducing its effect on the salt dissociation and the ions transport.

As shown in Fig. 2, the ionic conductivities of CPE-0, CPE-1, and CPE-3 all increased with increase of temperature in the temperature range measured. The linear plots reveal that the ionic conductivity data followed the Arrhenius equation, $\sigma(T) = \sigma^0 \exp\{-Ea/RT\}$. The fact that the ion transport in CPE-0 followed Arrhenius equation is ascribed to the high salt in the polymer electrolyte, which is known as polymer in salt, as reported [27,28]. On the other hand, the ion transport in the CPE system involved not just the segmental movement of the polymer chains but also the filler added as found in other studies [19,29]. The Ea values calculated from the Arrhenius plots are listed in Table 2. It shows that the *Ea* values of CPE-1 and CPE-3 are about half of that of CPE-0, indicating that the ions can be activated more easily and transport faster in CPE-1 and CPE-3 between 30 and 80 °C than in CPE-0 due to the presence of SAP. This reveals that the charge carriers moved more freely in the composite polymer electrolyte with SAP than that without SAP and is attributed to the extra interactions between the charge carriers and SAP with high surface area, interconnected pores and high porosity, which provided more transporting sites and shorter pathway for transporting the charge carriers as reported by Xi et al. [30] and Hu et al. [31].

3.2. FT-IR spectroscopy

FT-IR spectroscopy was used to obtain the information of the interactions among PAN, $LiClO_4$, and SAP in CPE. The previous publications [32–34] reported that the change in the absorbance of ClO_4^- that appeared between 600 and 650 cm^{-1} reveals the dissociation of $LiClO_4$. The absorbance was deconvoluted into two contributions: the "free" anion, which does not interact directly with the lithium cation, at ~624 cm^{-1} and the contacted "ion-paired" anion at ~635 cm^{-1}. Accordingly, the curve fitting of a Gaussian–Lorentzian peak to the ClO_4^- absorbance region for CPE-0 and CPE-3 was applied and is shown in Fig. 3 and the corresponding peak area ratios of the vibration peaks deconvoluted are summarized in Table 3. As listed, the fraction of the free anions increased with increase of the SAP concentration, implying that addition of SAP reduced the amount of the Li^+ ClO_4^- ion pairs, i.e. increased the dissolution of $LiClO_4$ in the PAN/SAP composite matrix, consequently, increasing the charge carriers that would enhance the ionic conductivity of the CPE. Nevertheless, as the SAP loading exceeded 3 wt% the fraction of the free anions for the CPE was decreased. This is ascribed to the aggregation of the high loaded SAP, which decreased the SAP's surface area, consequently, reducing the interaction of SAP with the cation of the salt to separate with the anion.

On the other hand, because the structure of PAN involves only the simple C–C backbone and the C≡N side groups, the change in the C≡N vibration absorbance caused by the presence of the salt and/or the filler can provide important information regarding the change in the interactions related to the polymer-side chain in the CPE. Fig. 4 shows the FT-IR spectra of the C≡N vibration absorbance of PAN, CP-3, CPE-0 and CPE-3 between 2200 and 2300 cm^{-1}. It is seen that the absorbance of the CN vibration for CP-3, the composite of PAN and 3 wt% of SAP, was almost the same as that for the pure PAN membrane, implying that no interaction between the CN groups and SAP was found in CP-3. However, a shoulder absorbance, corresponding to the bonded C≡N vibration, is observed for the composites CPE-0 and CPE-3. According to the previous report [35], the absorbance of C≡N vibration was deconvoluted into two contributions, the unbonded C≡N between 2235 and 2250 cm^{-1}, and the bonded C≡N between 2255 and 2270 cm^{-1}, for the CPEs and shown in Fig. 5 for CPE-0 and CPE-3 as examples. As listed in Table 4, the percentage of the bonded C≡N groups decreased with increase of the SAP content. This suggests that the interaction between Li^+ and CN was suppressed due to the presence of the SAP particles, resulting in an enhancement of the ionic conductivity. The result is similar to the result obtained in the Al_2O_3-containing PAN/$LiClO_4$ CPEs [1].

Table 2
Ionic conductivities, activation energy and mechanical property of CPE-*x*.

	SAP (wt%)	σ at 30 °C (S cm^{-1})	*Ea* (kJ mol^{-1})[a]	Yield stress (kg cm^{-2})	Yield elongation (%)
CPE-0	0	0.48×10^{-4}	22.0	16	141
CPE-1	1	1.35×10^{-4}	10.5	21	140
CPE-3	3	6.00×10^{-4}	10.3	29	201

[a] The *Ea* values were obtained from the data of Fig. 2.

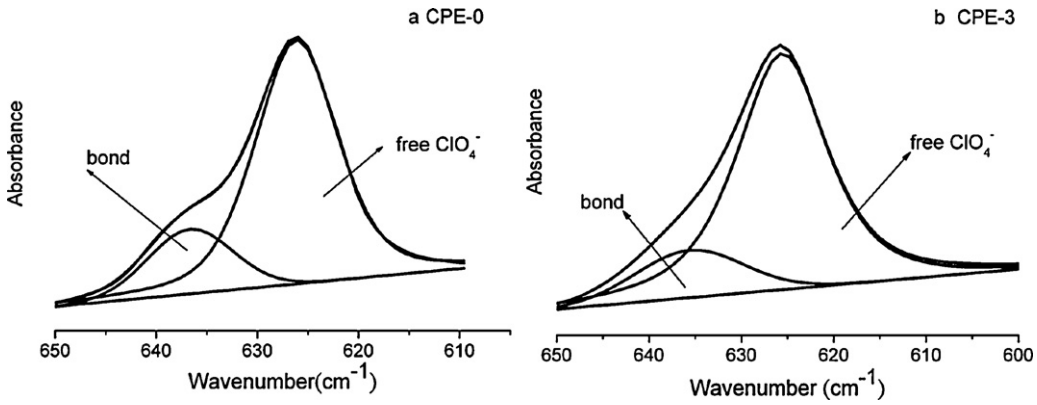

Fig. 3. Peak fitting of ClO_4^- absorbance for (a) CPE-0 and (b) CPE-3.

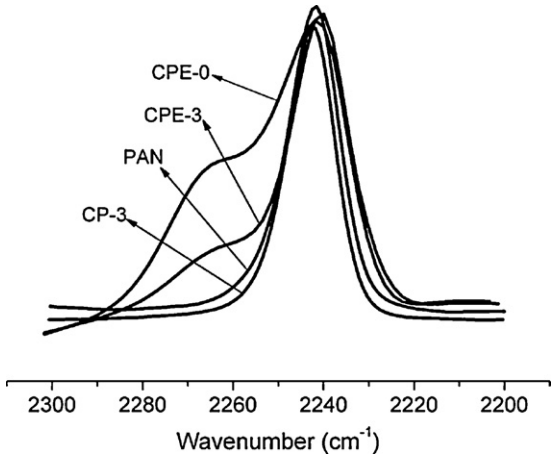

Fig. 4. FTIR spectra of C≡N absorbance for PAN, CP-3, CPE-0 and CPE-3.

Table 3
FT-IR peak positions and percentage of free ClO_4^- for CPE-*x*.

Sample	Free ClO_4^-		Bonded ClO_4^-	
	(cm^{-1})	(%)[a]	(cm^{-1})	(%)
CPE-0	626	80.2	636	19.8
CPE-1	625	80.9	637	19.1
CPE-2	626	82.2	635	17.8
CPE-3	626	83.7	637	16.3
CPE-4	626	81.1	637	18.9

[a] The percentage of the free ClO_4^- measured from the area ratio of the deconvoluted ClO_4^- peaks.

Table 4
FT-IR peak positions and percentage of C≡N for CPE-*x*.

Sample	Unbonded C≡N		Bonded C≡N	
	(cm^{-1})	(%)	(cm^{-1})	(%)
CPE-0	2239	42.7	2258	57.3
CPE-1	2239	50.2	2255	49.8
CPE-2	2238	55.8	2258	44.2
CPE-3	2238	65.0	2258	35.0
CPE-4	2239	60.4	2252	39.6

In addition, as shown in Fig. 6, a peak at about 1662 cm^{-1} was observed and assigned to the C=O vibration of DMF, indicating the presence of the DMF solvent residual. The lower frequency for the electrolytes than for the pure DMF (1685 cm^{-1}) is ascribed to the interaction with the Li^+. Besides, it is also found that the intensities of the C=O absorptions are similar for CPE-0 and CPE-3, revealing that the interaction between C=O of DMF and Li^+ was not changed after addition of SAP. Therefore, it is considered that the solvent effect in CPE-0 and CPE-3 were similar.

In all, the FTIR spectra indicate that the residual solvent effect was similar in CPE-0 and CPE-3, while the interaction between Li^+ and CN groups was suppressed due to the presence of the SAP particles. Besides, it also reveals that the dissolution of the $LiClO_4$ salt was increased in the SAP-containing CPEs, implying that the dissolution of lithium ion was achieved by coordinating with the residual DMF, PAN chain as well as SAP in CPEs.

3.3. Solid-state NMR

^{7}Li MAS NMR with high power proton decoupling was used to investigate the coordination around the lithium ions of CPE-0 and

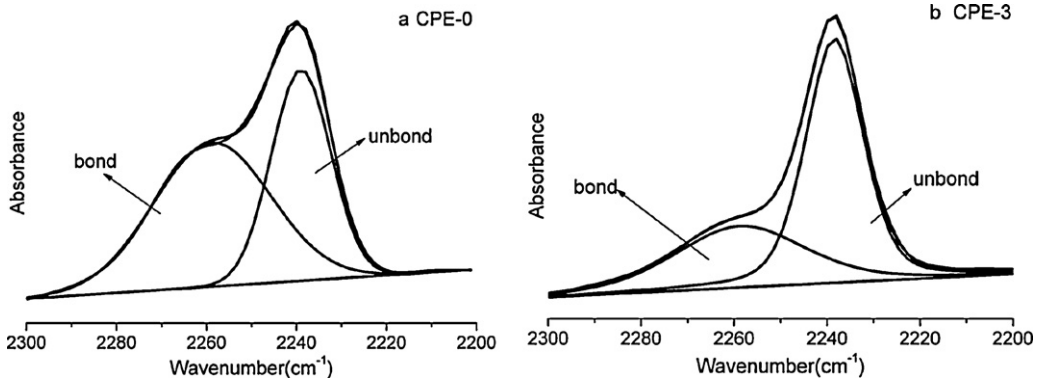

Fig. 5. Peak fitting of the C≡N absorbance for (a) CPE-0 and (b) CPE-3.

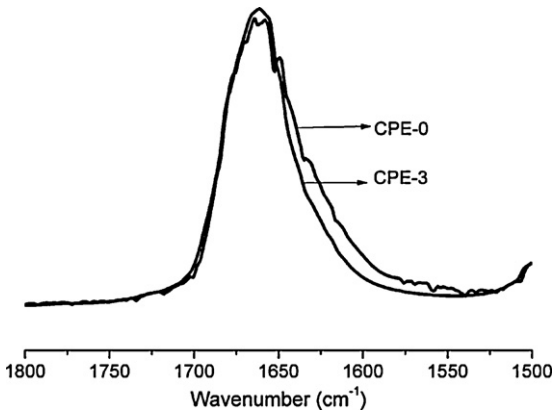

Fig. 6. FTIR spectra of C=O absorbance for CPE-0 and CPE-3.

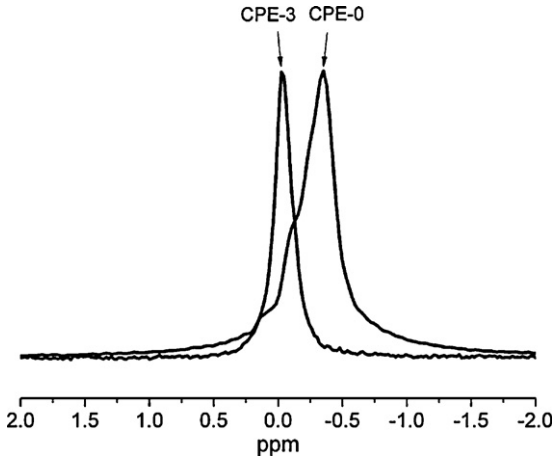

Fig. 7. Solid state ^{7}Li MAS NMR of CPE-0 and CPE-3.

CPE-3. The spectra are shown in Fig. 7 and the corresponding data are summarized in Table 5. It is found that the ^{7}Li chemical shift (in ppm) was significantly increased from −0.35 ppm to −0.03 ppm after addition of SAP, which is very close to 0 ppm, the chemical shift of the free lithium ion in the aqueous LiCl solution, i.e. the Li^+ ions in CPE-3 were less shielded and their environments were more similar to that in the aqueous LiCl solution than that in CPE-0. This reveals that due to the presence of SAP the Li^+ ions in CPE-3 were in a freer ionic configuration than in CPE-0 and could migrate as free as that in the aqueous LiCl solution. Besides, the half width (defined by the full width at half height of the main peak, FWHM) of an NMR peak is known to reflect the ion mobility in the polymer electrolyte system. As indicated in Table 5, the FWHM for CPE-3 is much smaller than that for CPE-0, confirming that the mobility of the Li^+ ions in CPE-3 was higher than that in CPE-0 [36,37]. The NMR results suggest that in SPE-3 there were coordination between Li^+ ions and SAP as revealed by the FTIR results discussed above.

Table 5
^{7}Li NMR data of the CPE-0 and CPE-3.

Sample	Chemical shift (ppm)	FWHM (ppm)
CPE-0	−0.35	0.30
CPE-3	−0.03	0.15

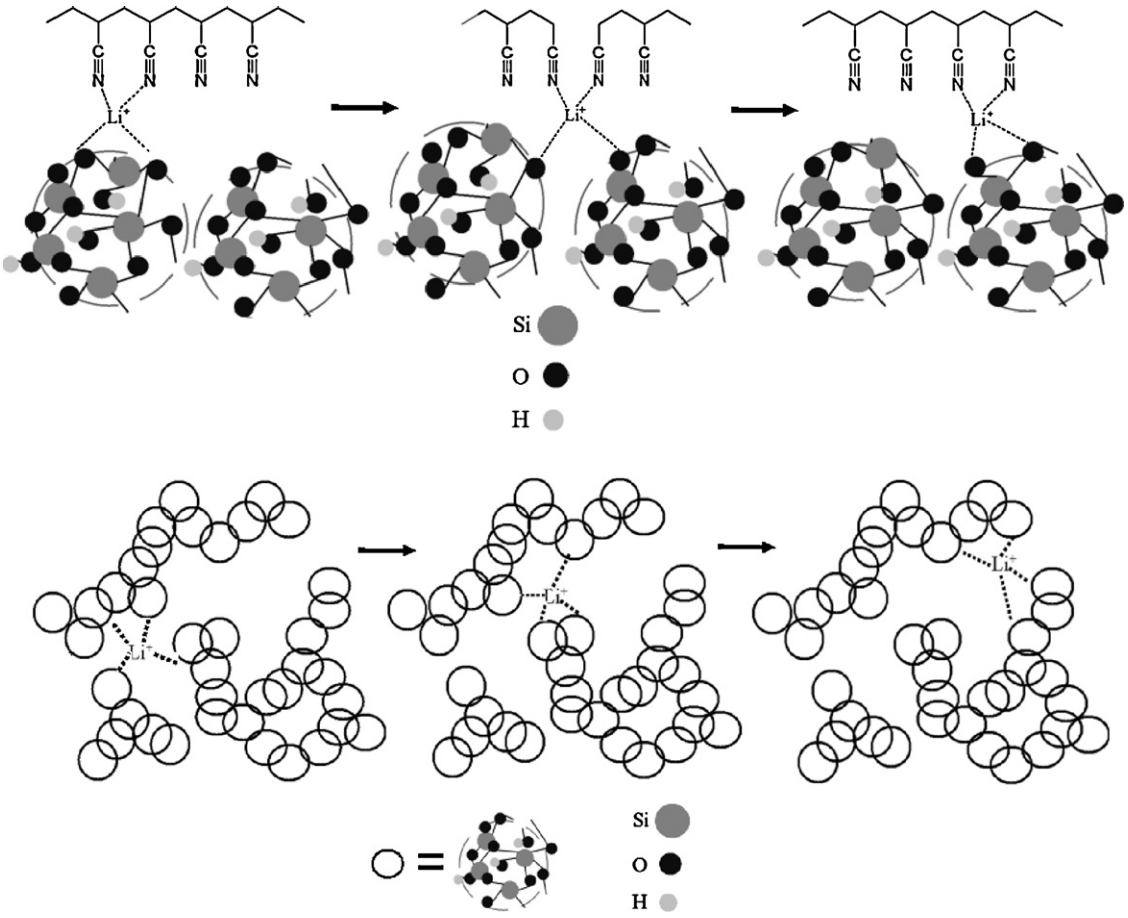

Fig. 8. The proposed conduction mechanism of the lithium ion in CPE.

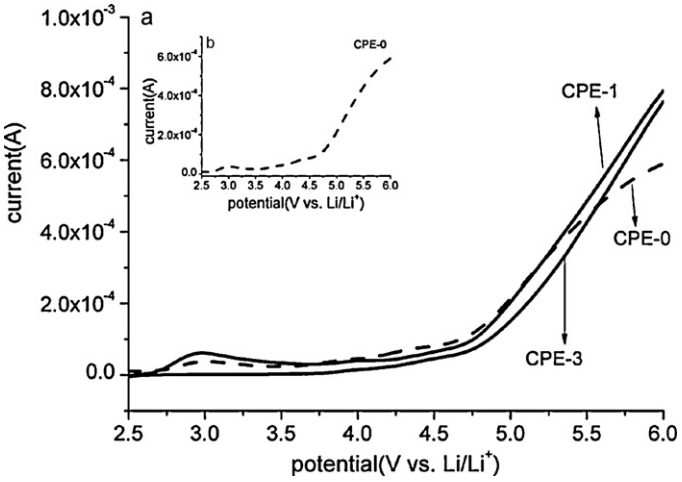

Fig. 9. Linear sweep voltammograms of CPE-*x*.

According to the FT-IR and NMR results, except hopping through the polymer chains, well known for the polymer electrolyte, the lithium ion conduction mechanism involving the SAP particles in CPE prepared may be proposed as following. As indicated in Fig. 8, the Li^+ ions might migrate through (1) the PAN–SAP interface with the possible complexes formed by weakly coordinating to the C≡N groups of PAN and the Lewis-base sites, the Si–O–Si sites on the exterior surface of SAP, and (2) the vacancies of SAP, which provided a shorter path with the possible complexes formed by weakly coordinating to the Si–O–Si sites on the interior surface of the SAP mesopores.

3.4. Mechanical property

With the improvement in ionic conductivity by addition of SAP, preserving the mechanical strength is important for CPE as well. However, for most of the polymer electrolytes an enhancement of conductivity usually leads to a reduction of the mechanical stability and vice versa. Therefore, few mechanical property data of the conductive polymer electrolytes have been reported. Nevertheless, the CPEs prepared in this study were strong enough for measurement. As can be seen in Table 2, the yield stress of CPE was increased with increasing the SAP content and about 201% of yield elongation was obtained for CPE-3 which could result in a better contact with the electrodes than CPE-0. This result also supports that the CPE membranes prepared were solid type polymer electrolytes.

3.5. Electrochemical stability

The electrochemical stability of the composite polymer electrolyte films were studied by the linear sweep voltammetry and cyclic voltammetry analyses. As can be seen in Fig. 9(b), the voltage breakdown of CPE-0 occurred at about 3.5 V, while that of CPE-1 and CPE-3 occurred at about 4.5 V, indicating that the PAN/$LiClO_4$ polymer electrolyte was electrochemically stable up to 4.5 V due to addition of SAP. This implies that all the SAP-containing CPEs had a higher anodic stability than CPE-0 and met the requirement for application in lithium polymer battery.

In addition, the electrochemical stabilities of CPE-0 and CPE-3 were investigated by the cyclic voltammetry analysis between 0 V to 4 V for the cells fabricated with CPE-0 and CPE-3. The CV curves of the first 50 cycles for CPE-0 and CPE-3 are displayed in Fig. 10(a) and (b), respectively. As can be seen, the Li stripping occurred at 2.2 V (oxidation process) and the deposition took place at 1.7 V

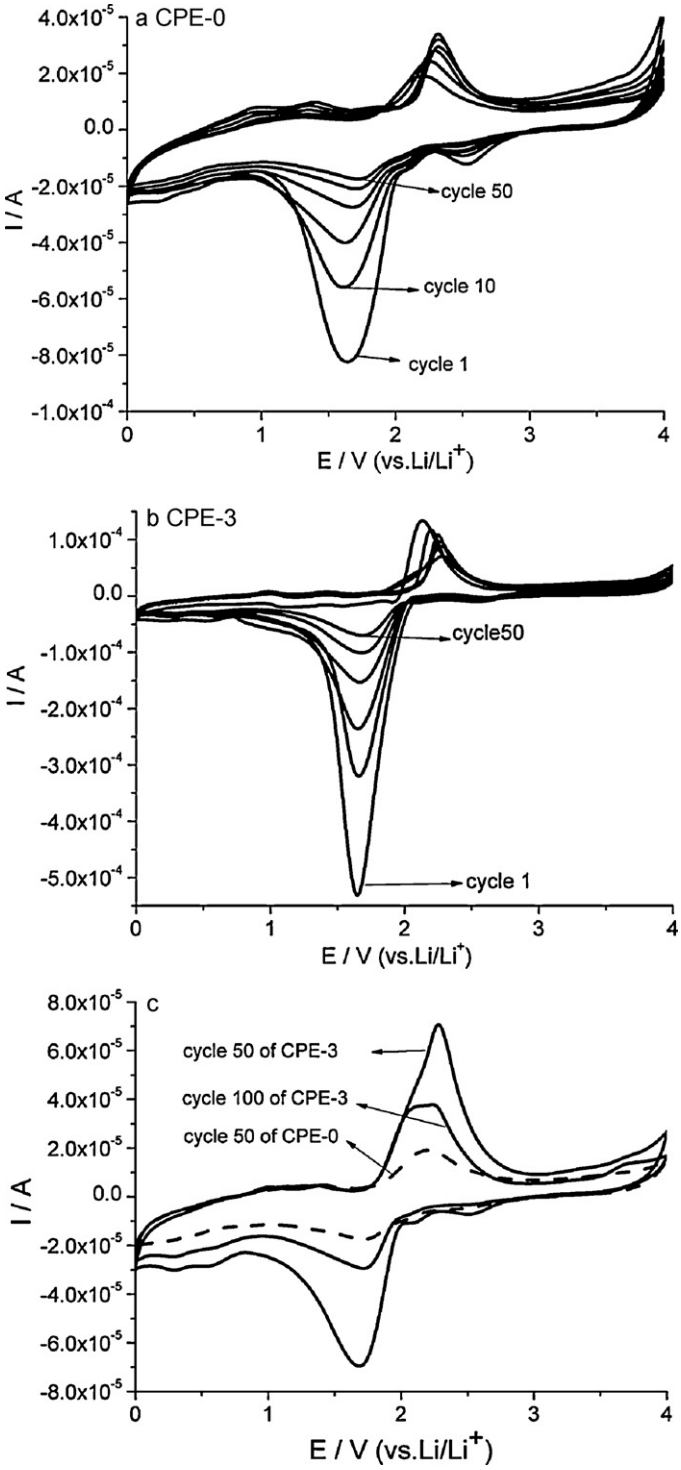

Fig. 10. Cyclic voltammograms of (a) CPE-0 for first 50 cycles, (b) CPE-3 for first 50 cycles, (c) cycle 50 of CPE-0, cycle 50 and cycle 100 of CPE-3.

(reduction process), which is higher due to the poor interface between the solid type electrolyte and the Pt electrode than the liquid or gel type electrolytes. Besides, it was also possible caused by that the Pt was mounted on an SS substrate of the measurement assembly and the Li–Pt alloy was probably formed, of which a detail investigation is needed in the future work. Nevertheless, it is found that under the same measurement condition, the peak current of CPE-3 was much higher than that of CPE-0 for all the cycles and the peak current of cycle100 for CPE-3 was even higher than that of cycle 50 for

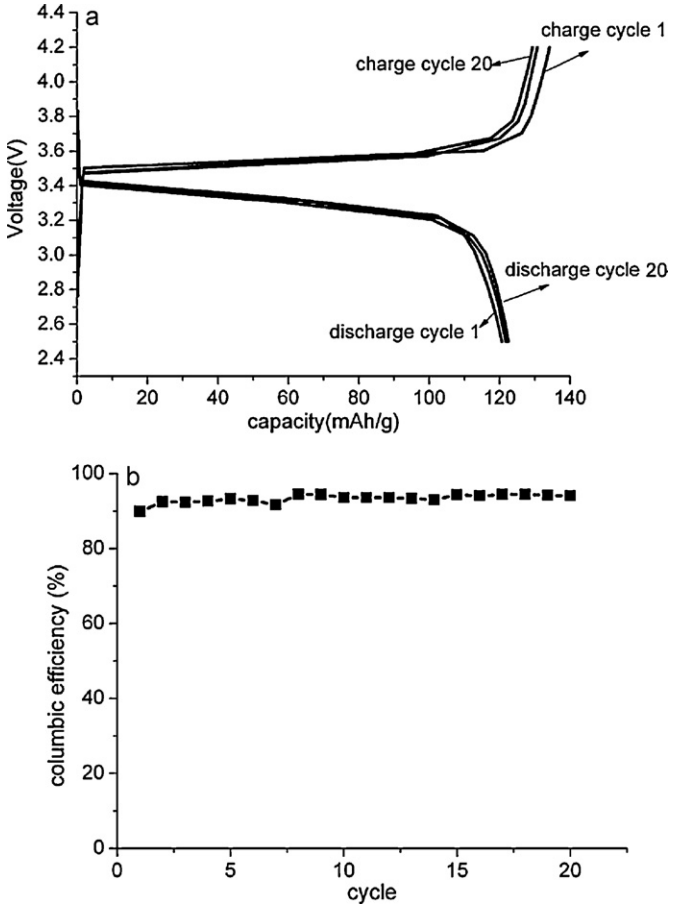

Fig. 11. Charge/discharge curves and columbic efficiency of Li/CPE-3/$LiFePO_4$ battery vs. cycle number at room temperature. The test was carried out at discharge rate of 0.5 C within the voltage range of 2.5–4.2 V.

CPE-0 as indicated by Fig. 10(c), revealing that CPE-3 had better electrochemical stability and cyclability than CPE-0 between 0 V and 4 V. This is ascribed to that the lithium ion's mobility was higher in CPE-3 than CPE-0 due to the extra transport paths provided by SAP as discussed above.

3.6. Charge–discharge capacity

The charge/discharge curves of the coin cell fabricated with CPE-3 were shown in Fig. 11(a). This coin cell delivered a discharge capacity of 120, 122 and 121 mAh g^{-1} at 0.5 C rate for the first, tenth and twentieth charge/discharge cycle, respectively. After 20 cycles, the coin cell still retained about 100% of the initial discharge capacity. As shown in Fig. 11(b) the columbic efficiency, the ratio of discharge capacity to charge capacity, was 89.9%, 93.6% and 94.1% for the first, tenth and twentieth cycle, respectively. This suggests that CPE-3 was quite stable in the charge–discharge process and the possible passivated film on the anode and the cathode surface to cause charge transfer difficulties were efficiently suppressed.

4. Conclusions

This study demonstrated that dispersing the silica aerogel powder (SAP) into the PAN/$LiClO_4$ polymer electrolyte made the composite a better polymer electrolyte than that without SAP. The results showed that due to the presence of SAP the over all dissolution percentage of the $LiClO_4$ salt was higher and the Li^+ ions could migrate more freely in CPE than in CPE-0, resulting in higher ionic conductivity. This is ascribed to that the interaction of Li^+ and C≡N was weakened due to the possible coordination of Li^+ with SAP, which also assisted to dissolve the $LiClO_4$ salt. Besides, as the proposed conduction mechanism, the Li^+ ions not only could transport by the conventional hopping way through the polymer chains, but also could migrate through the SAP–PAN interface and the vacancies in SAP by the formation of the possible complexes. The presence of SAP not only increased the concentration of the solvated Li^+, the interconnected mesopores of SAP with high surface area and high porosity also provide more transporting sites and shorter pathway, resulting in increasing the mobility of the Li^+ ions in the electrolyte. Therefore, the ionic conductivity of the SAP-containing polymer electrolyte was enhanced. The ionic conductivity of the PAN/$LiClO_4$/SAP composite polymer electrolyte was increased about 12.5 times when 3 wt% of SAP was added to the composite. The results of the cyclic voltammetry measurements showed that the anodic and cathodic peaks were well maintained after 100 cycles, confirming that CPE-3 had excellent electrochemical stability and cyclability over the potential range between 0 V and 4 V vs. Li/Li^+. Besides, the charge–discharge of the coin cell fabricated with CPE-3 showed that the discharge capacity of the coin cell was about 120 mAh g^{-1} and after 20 charge–discharge cycles the coin cell still retained almost 100% of the initial discharge capacity.

Acknowledgments

The authors would like to thank the National Science Council (NSC098-2811-M-033-002) of the R.O.C. and Chung Yuan Christian University, ROC (CYCU-98-CR-CH) for providing financial support to this research work.

References

[1] Y.W. Chen-Yang, H.C. Chen, F.J. Lin, C.C. Chen, Solid State Ionics 150 (2002) 327–335.
[2] I.D. Wu, F.C. Chang, Polymer 48 (2007) 989–996.
[3] J. Xi, X. Qiu, M. Cui, X. Tang, W. Zhu, L. Chen, J. Power Sources 156 (2006) 581–588.
[4] J.W. Kim, K.S. Ji, J.P. Lee, J.W. Park, J. Power Sources 119/121 (2003) 415–4121.
[5] H. Zhang, P. Maitra, S.L. Wunder, Solid State Ionics 178 (2008) 1975–1983.
[6] T.K.J. Köster, L.v. Wüllen, Solid State Ionics 181 (2010) 489–495.
[7] M.Y.A. Rahman, A. Ahmad, L.H.C. Ismail, M.M. Salleh, J. Appl. Polym. Sci. 115 (2010) 2144–2148.
[8] Z.M. Dang, L.Z. Fan, S.J. Zhao, C.W. Nan, Mater. Res. Bull. 38 (2003) 499–507.
[9] H.M. Xiong, X. Zhao, J.S. Chen, J. Phys. Chem. B 105 (2001) 10169–10174.
[10] Y.W. Chen-Yang, Y.T. Chen, H.C. Chen, W.T. Lin, C.H. Tsai, Polymer 50 (2009) 2856–2862.
[11] Q.T. Ngyen, D.G. Baird, Adv. Polym. Technol. 25 (2006) 270–285.
[12] J.J. Hwang, H.J. Liu, Macromolecules 35 (2002) 7314–7319.
[13] H.M. Kao, C.L. Chen, Angew. Chem. Int. Ed. 43 (2004) 980–984.
[14] H.M. Kao, S.W. Chao, P.C. Chang, Macromolecules 39 (2006) 1029–1040.
[15] S. Kim, S.J. Park, Electrochim. Acta 52 (2007) 3477–3484.
[16] J. Xia, X. Qiua, W. Zhua, X. Tang, Micropor. Mesopor. Mater. 88 (2006) 1–7.
[17] C.V. Subba Reddy, G.P. Wu, C.X. Zhao, Q.Y. Zhu, W. Chen, R.R. Kalluru, J. Non-Cryst. Solids 353 (2007) 440–445.
[18] J.Y. Xi, X.P. Qiu, X.M. Ma, M.Z. Cui, J. Yang, X.Z. Tang, W.T. Zhu, L.Q. Chen, Solid State Ionics 176 (2005) 1249–1260.
[19] Y.W. Chen-Yang, Y.L. Wang, Y.T. Chen, Y.K. Li, H.C. Chen, H.Y. Chiu, J. Power Sources 182 (2008) 340–348.
[20] F. Croce, R. Cuini, A. Matinelli, L. Persi, F. Ronci, B. Scrosati, J. Phys. Chem. B 103 (1999) 10632–10638.
[21] S.H. Chung, Y. Wang, L. Persi, F. Croce, S.G. Greenbaum, B. Scrosati, E. Plichta, J. Power Sources 97–98 (2001) 644–648.
[22] P.A.R.D. Jayathilaka, M.A.K.L. Dissanayake, I. Albinsson, B.E. Mellander, Elctrochim. Acta 47 (2002) 3257–3268.
[23] M. Marcinek, A. Bac, P. Lipka, A. Zalewska, G. Zukowska, R. Borkowska, W. Wieczorek, J. Phys. Chem. B 104 (2000) 11088–11093.
[24] M.J. Reddy, P.P. Chu, J. Power Sources 135 (2004) 1–8.
[25] M.R. Ayers, A.J. Hunt, J. Non-Cryst. Solids 285 (2001) 123–127.
[26] L.W. Hrubesh, J. Non-Cryst. Solids 225 (1998) 335–342.
[27] C.A. Angell, C. Liu, E. Sanchez, Nature 362 (1993) 137–139.
[28] M. Forsyth, S. Ji, D.R. MacFarlance, A.J. Hill, J. Polym. Sci. Part B: Polym. Phys. 38 (2000) 341–350.
[29] M. Forsyth, S. Ji, D.R. MacFarlance, Solid State Ionics 112 (1998) 161–163.
[30] J.Y. Xi, S.J. Mao, X.Z. Tang, Macromolecules 37 (2004) 8592–8598.

[31] L. Hu, Zi.g. Tang, Z. Zhang, J. Power Sources 166 (2007) 226–232.
[32] W. Wieczorek, A. Zalewska, D. Raducha, Z. Florjan'czyk, J.R. Stevens, J. Phys. Chem. B 102 (1998) 352–360.
[33] M. Salomon, M. Xu, E.M. Eyring, S. Petrucci, J. Phys. Chem. 98 (1994) 8234–8244.
[34] W. Wieczorek, P. Lipka, G. Zukowska, H. Wycislik, J. Phys. Chem. B 102 (1998) 6968–6974.
[35] B. Huang, Z. Wang, L. Chen, R. Xue, F. Wang, Solid State Ionics 91 (1996) 279–284.
[36] M. Forsyth, D.R. MacFarlane, A. Best, J. Adebahr, P. Jacobsson, A.J. Hill, Solid State Ionics 147 (2002) 203–211.
[37] J. Adebahr, A.S. Best, N. Byrne, P. Jacobsson, D.R. MacFarlane, M. Forsyth, Phys. Chem. Chem. Phys. 5 (2003) 720–725.